Sains Malaysiana 52(11)(2023): 3253-3260
http://doi.org/10.17576/jsm-2023-5211-17

The Characteristic of pH Sensing of Potentiometric on Zinc Oxide and Aluminium-Doped Zinc Oxide Nanostructures

(Ciri Penderiaan pH Potensiometrik pada Nanostruktur Zink Oksida dan Zink Oksida Terdop Aluminium)

Ain Zafirah Kamaruddin[1], Lim Kar Keng[2,*], Muhammad Azmi Abdul Hamid[1], Naif H. Al-Hardan[1], Huda Abdullah[3] & Ensaf Mohammed Al-Khalqi[4]

[1]*Department of Applied Physics, Faculty of Science and Technology, Universiti Kebangsaan Malaysia, 43600 UKM Bangi, Selangor, Malaysia*
[2]*School of Liberal Studies, Universiti Kebangsaan Malaysia, 43600 UKM Bangi, Selangor, Malaysia*
[3]*Department of Electrical, Electronics and System Engineering, Faculty of Engineering and Built Environment, Universiti Kebangsaan Malaysia, 43600 UKM Bangi, Selangor, Malaysia*
[4]*Physics Department, Faculty of Applied Science, Thamar University, 87246 Dhamar, Yemen*

Received: 11 May 2023/Accepted: 18 October 2023

ABSTRACT

Numerous investigations have been conducted to increase the sensitivity and stability of metal oxide semiconductors as pH-sensing membranes. This paper will describe the pH sensing and characterisation of zinc oxide (ZnO) and aluminium-doped zinc oxide (ZnO:Al) as potentiometric pH sensors. The hydrothermal technique was used to grow ZnO and ZnO:Al thin film nanostructures with doping concentrations of 1, 3, and 5 at% Al on the cleaned ITO substrates. The pH potentiometric sensing was performed in a wide pH range of 4-12 and produced sensitivity, including stability of the nanostructures. The prepared samples were also characterized by X-ray diffraction analysis (XRD), field effect scanning electron microscope (FESEM), and energy dispersive X-ray (EDX) to explore the influence of aluminium concentration on structural and morphology characteristics and then prepared as electrodes for pH sensing. From the XRD result, the sharp peaks and high peak intensities demonstrated well crystalline of the synthesized ZnO nanorods. Furthermore, the FESEM shows the growth of array nanorods perpendicular over the surface of ITO. The sensitivity of the pH sensor with 3 at% ZnO:Al exhibits higher sensitivity (43.80 mV/pH) and larger linearity (0.9507).

Keywords: Aluminium-doped zinc oxide; doping process; hydrothermal process; pH-sensing; ZnO nanostructures

ABSTRAK

Banyak kajian telah dijalankan untuk meningkatkan sensitiviti dan kestabilan semikonduktor oksida logam sebagai membran penderia pH. Kertas ini akan menerangkan penderiaan pH dan pencirian zink oksida (ZnO) serta zink oksida terdop aluminium (ZnO:Al) sebagai penderia pH potensiometrik. Teknik hidroterma digunakan untuk menumbuhkan nanostruktur filem nipis ZnO dan ZnO terdop Al (ZnO:Al) dengan kepekatan dopan 1, 3 dan 5 at% di atas substrat ITO yang telah dibersihkan. Penderiaan pH potensiometrik dilakukan dalam julat pH yang luas iaitu 4-12 dan menghasilkan sensitiviti termasuk kestabilan nanostruktur. Sampel yang disediakan juga dicirikan oleh analisis pembelauan sinar-X (XRD), mikroskop elektron pengimbasan kesan medan (FESEM), sinar-X penyebaran tenaga (EDX) untuk meneroka pengaruh kepekatan aluminium terhadap ciri-ciri struktur dan morfologi dan kemudian disediakan sebagai elektrod untuk pengesanan pH. Daripada keputusan XRD, kemuncak tajam dan keamatan puncak yang tinggi menunjukkan hablur nanorod ZnO disintesis dengan baik. Tambahan pula, FESEM mendedahkan pertumbuhan tatasusunan nanorod berserenjang di atas permukaan ITO. Sensitiviti penderia pH pada 3 at% ZnO:Al menunjukkan sensitiviti yang lebih tinggi (43.80 mV/pH) dan lineariti yang lebih besar (0.9507).

Kata kunci: Kaedah hidroterma; nanostruktur ZnO; pengesanan pH; proses pengedopan; zink oksida terdop aluminium

Introduction

At ambient temperature, zinc oxide is an excellent n-type semiconductor with a high and direct energy bandgap (3.37 eV), thermal stability at room temperature, non-toxicity, and can be prepared at the effective low-cost process (Liu et al. 2017; Porwal, Shafi & Sahu 2022; Young, Lai & Tang 2019). Due to its extraordinary chemical, optical, magnetic, electronic, stable, and biocompatible capabilities, ZnO has been a hot topic in the study (Al-Khalqi et al. 2021b; Belkhaoui et al. 2019; Ghazai, Salman & Jabbar 2016). Recently, several research studies have reported the development of metal oxide semiconductor material with potential as a pH sensor element. In comparison to other metal oxides, ZnO was selected as a favourable material in various applications such as solar cells, biomedical, optoelectronic devices, and including the development of biosensors (Al-Hardan et al. 2017; Al-Khalqi et al. 2022; Hashim et al. 2017). Nevertheless, the conductivity of the ZnO thin film is poor, and doping ZnO with other elements may increase it (Ahmed 2018). Based on Agarwal et al. (2020), Al Farsi et al. (2021), and Al-Hardan et al. (2021), aluminium has been the most widely utilised dopant element since the process is cost-effective and can improve the electrical properties by increasing the conductivity of ZnO. Additionally, the device structure of epitaxial and superlattice design, which may minimise losses at layer interfaces and hence increase device performance, has an evident advantage for material structures like ZnO and aluminium-doped zinc oxide (Naik et al. 2012; Zhang et al. 2013; Zheng et al. 2018). Moreover, according to Mishra, Mishra and Pathak (2022), Peng et al. (2015), and Wang et al. (2013), the process of producing doped ZnO nanorods may be carried out using a variety of techniques, including chemical bath deposition (CBD), spray pyrolysis, magnetron sputtering, sol-gel, and hydrothermal approach. Among all the methods, hydrothermal process is the preferred and versatile method as it is simple, low-cost fabrication, and environmentally friendly with repeatable results (Kumar A. et al. 2019; Vavale et al. 2018; Yue et al. 2019). The physical and optical characteristics of ZnO and ZnO:Al have been the subject of several studies (Ahmed 2018; Alkahlout et al. 2014; Ghazai, Salman & Jabbar 2016), but only a small number of papers have focused on pH sensing and characterization, which primarily affect electrochemical and biosensor. In this work, we investigated the effects of Al doping of hydrothermal growth of ZnO and ZnO:Al at 1, 3 and 5 at%. Field effect scanning electron microscopy (FESEM), X-ray diffraction (XRD), and energy-dispersive X-ray (EDX) spectroscopy were used to characterise the morphology and elemental composition of the ZnO and ZnO:Al nanorods. The sensitivity and linearity of the pH-sensing sensor will be discussed in depth. In addition, a comparison between the sensitivity and drift of pH sensors of various measurement methods will be presented, giving particular attention to materials and technology (Table 1).

Materials and Methods

In general, acetone, methanol, and ethanol were used to clean conductive glass ITO, followed by cleaning with deionized water (DIW) using an ultrasonic method. ZnO and ZnO:Al nanorods were produced using the hydrothermal technique. The precursor solution was created by mixing 0.025 M hexamethylenetetramine (HMTA) and 0.025 M zinc nitrate hexahydrate ($Zn(NO_3)_2 \bullet 6H_2O$). Similar procedures were followed, with the addition of aluminium nitrate nanohydrate ($Al(NO_3)_2 \bullet 9H_2O$) for the growth of Al-doped ZnO into precursor solution. Al dopant's atomic ratio was designated as ZnO:Al (1%), ZnO:Al (3%), and ZnO:Al (5%), respectively. The growth procedure was placed over 6 h in a standard oven at 95 °C. The samples were then cooled to room temperature and rinsed with deionized water. The samples have been dried in a conventional oven for 20 min at 100 °C. Following the steps outlined in Yue et al. (2019), the samples were then produced as an electrode. Before the detecting membranes were tested, the manufactured pH sensors were submerged in reverse osmosis (RO) water for 12 h. For 20 min, the prepared electrode was submerged in a pH 7 buffer solution. After that, the electrode was immersed in a pH 7 buffer solution for 10 min before the experiment began. In order to prevent any interference on the surface of prepared electrode, it was immersed in deionized water (DIW) between each measurement of the buffer solution. The electromotive force (emf) was measured with a high input impedance operational amplifier (Op-amp). The CA3140 Op-amp (Renesas Electronics Corporation, Japan) was utilised as a voltage follower with an unity gain output. The working electrode (WE) was connected to the non-inverted (+) input terminal of the Op-amp and Ag/AgCl acting as reference electrode (RE). An Agilent 34410A digital multimeter (Agilent Technologies Sales (M) Sdn. Bhd. Malaysia) were connected to the Op-amp output. Then, the multimeter was controlled by a PC through the USB port. The measurement was set up using a customised LabView programme, and the data were recorded for subsequent analysis. The measurements were performed at 23 °C ± 1 °C and a humidity of 51%. Figure 1 illustrates the way this work was set up.

TABLE 1. Comparison of pH sensor in different measurement method

Based compound	Doping percentage (at%)	Sensitivity (mV/pH)	Drift (mV/h)	pH range	Measurement method	Reference
ZnO doped with Al	0% 1% 3% 5%	26.03 29.84 43.80 30.99	7.97 3.43 2.82 16.21	pH 4 - 12	Potentiometric	Current
ZnO doped with Al	0% 1% 2% 3% 5% 7%	35.23 49.79 54.16 57.95 55.61 53.34	16.81 13.59 4.77 1.27 3.38 8.79	pH 1 - 13	MOSFET	pH-Sensing Characteristics of Hydrothermal Al-Doped ZnO Nanostructures (Wang et al. 2013)
ZnO doped with Al	0% 1.98% 3.35% 6.27%	35.23 57.95 55.61 53.34	-	pH 1 -13	EGFET	pH Sensing Characteristics of Extended-Gate Field-Effect Transistor Based on Al-Doped ZnOanostructures Hydrothermally Synthesized at Low Temperatures (Yang et al. 2011)
ZnO Doped with Al	0% 1%	26.70 42.99	2.88 2.24	pH 2 - 10	Potentiometric	ZnO and AZO Film Potentiometric pH Sensors Based on Flexible Printed Circuit Board (Yang, Chang & Chan 2022)

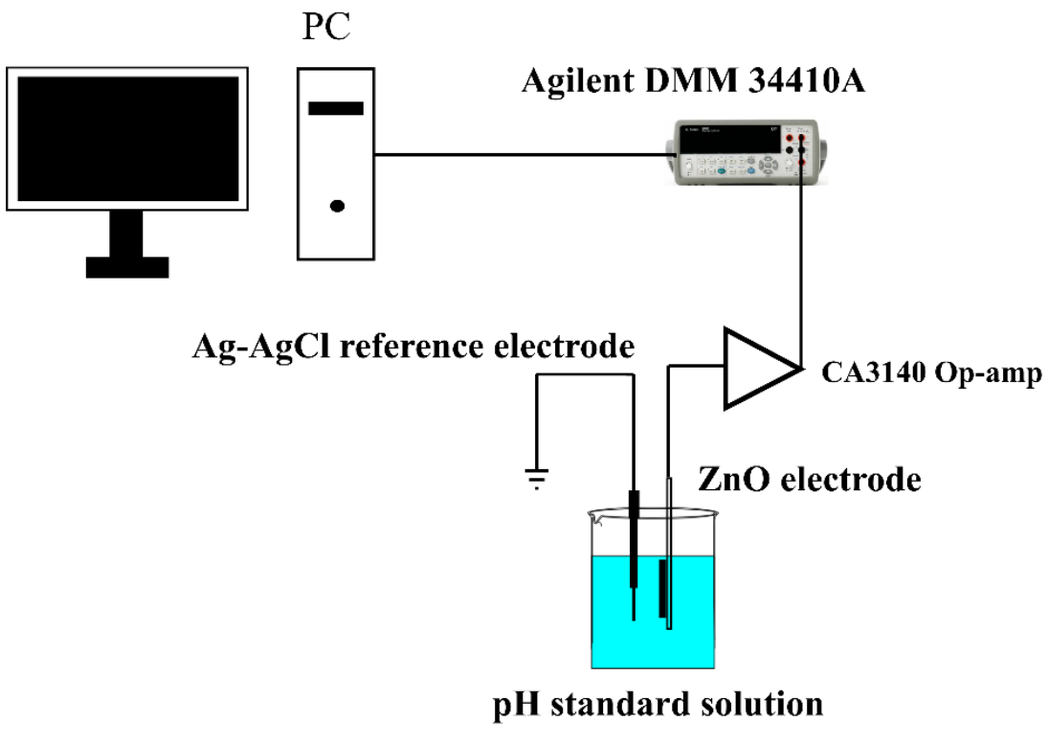

FIGURE 1. The experiment setup to measure potential difference between working and reference electrode

Results and Discussion

Figure 2 shows the X-ray diffraction (XRD) pattern of the produced ZnO and ZnO:Al NRs. It summarizes the fundamental information of ZnO crystalline structures as analyzed from the pattern. All produced materials were analysed using the Bruker D8 Advance XRD equipment in the diffraction angle range of 20-80 degree using Cu Kα radiation (λ = 1.5405 Å). The diffraction peaks indicate the presence of a wurtzite-structured hexagonal phase of ZnO. These nanorods are extremely pure, as no secondary phase belonging to other elements could be found. All of the diffraction peaks in Figure 2 can be well indexed with the ZnO hexagonal wurtzite structure (JCPDS 036-1451).

The crystalline nature of the prepared powders shows the same structure quality even after doping with 1, 3, and 5 at% Al. This result may be due to the presence and enhancement of the aluminium doping towards nanorods ZnO. However, the intensity of the (002) peak was found to particularly begin to decrease when doping reaches 1, 3, and 5 at%, which is probably as a result of the ZnO structure being destruction and reorganized (Al-Hardan et al. 2021). Besides, Figure 2 also shows the diffraction peaks that correlate to the ITO substrate. In accordance with the XRD results, strongly orientated ZnO nanorods were produced perpendicular to the substrate surface. Furthermore, no significant difference in peak position was detected between ZnO thin films and ZnO:Al indicating that Al can be incorporated into ZnO without causing stress due to ion size differences between Al and Zn (Ghazai, Salman & Jabbar 2016; Mishra, Mishra & Pathak 2022). All the peaks at 2θ values show 34.4° corresponding to the plane [002].

Figure 3 shows the surface morphology of ZnO and ZnO:Al nanorods grown on ITO conductive glass. Based on Figure 3(a), the images of ZnO show the clear presence of hexagonal nanorods, confirming a c-axis growth by hydrothermal method at 95 °C along the [002] direction. When the ZnO:Al doping concentration is increased by 1% and 3%, the flawless hexagonal form of the nanorods morphology begins to disappear. The enhancement of Al doping exhibits nanorod hexagonal shape, and some nanorods grow at random angles in some particular regions. As the ZnO:Al (5%), there was a decreased amount of hexagonal nanorods form; unfortunately, several nanosheets of ZnO have been seen. Similar results were obtained using ZnO nanorods, which took on a disordered orientation and were tightly packed with overlapping rods (Kim et al. 2000). To verify the purity and the elemental compositions of produced ZnO and ZnO:Al, energy-dispersive X-ray (EDX) spectroscopy is utilised. The ZnO and ZnO:Al nanostructures are composed of Zn, O, and Al, as shown by the several well-defined peaks in the EDX spectrum that were clearly associated with Zn, O, and Al. There were no further impurity-related peaks in the EDX spectra.

As a function of pH buffer values in the range of 4 to 12, which includes both the acidic and alkaline environment, Figure 4 shows the differential potentiometric response of the synthesized ZnO and ZnO:Al. According to binding sites theory, the membrane surface was protonated or deprotonated during the chemical interaction between the sensing surface and the pH buffer solution, leading the sensor to produce various response voltages in solutions with various pH values (Yang, Chang & Chan 2022). Figure 4 depicts the sensitivity and linearity of ZnO and ZnO:Al (1%), ZnO:Al (3%), and ZnO:Al (5%) based on pH sensor response voltage (mV) versus different pH values. The sensitivity for the ZnO was 26.03 mV/pH with linearity of 0.9576. However, the sensitivity was enhanced for ZnO:Al (1%) at 29.84 mV/pH with a linearity of 0.8676, ZnO:Al (3%) was 43.80 mV/pH, linearity of 0.9507 while the sensitivity for ZnO:Al (5%) was 30.99 mV/pH with linearity 0.9399. These results show that the prepared pH sensor exhibits good and excellent linearity. However, the results also show that ZnO doped with 3 at% Al demonstrates high sensitivity and linearity, compared to the ZnO and ZnO:Al (1%) and ZnO:Al (5%). This kind of metal oxide film can build the pH sensor through a wide pH range. Furthermore, this finding is consistent with Rayathulhan, Sodipo and Aziz (2017), and Zhang et al. (2013) findings, where the sensitivity value increases from ZnO to ZnO:Al. Therefore, it proves that adding aluminum to ZnO can have a flexible sensor and increase the voltage response and stability of the pH sensor (Alkahlout et al. 2014; Yue et al. 2019). The improvement in Al doping of ZnO could be attributed to an enhancement of the site density that improves the reaction sight by increasing charge carriers (Vavale et al. 2018).

Drift or stability is described as the gradual change in sensor response over time while the pH value keeps in constant (Tsai et al. 2019). Long-term testing indicates drift in the ZnO, and ZnO:Al pH sensors. The prepared pH sensor was immersed in pH 7 buffer solution for 12 h, and analyzed the response voltage of pH sensor response using the pH sensor potentiometric measurement device. The surface potential of the sensing film changes as a

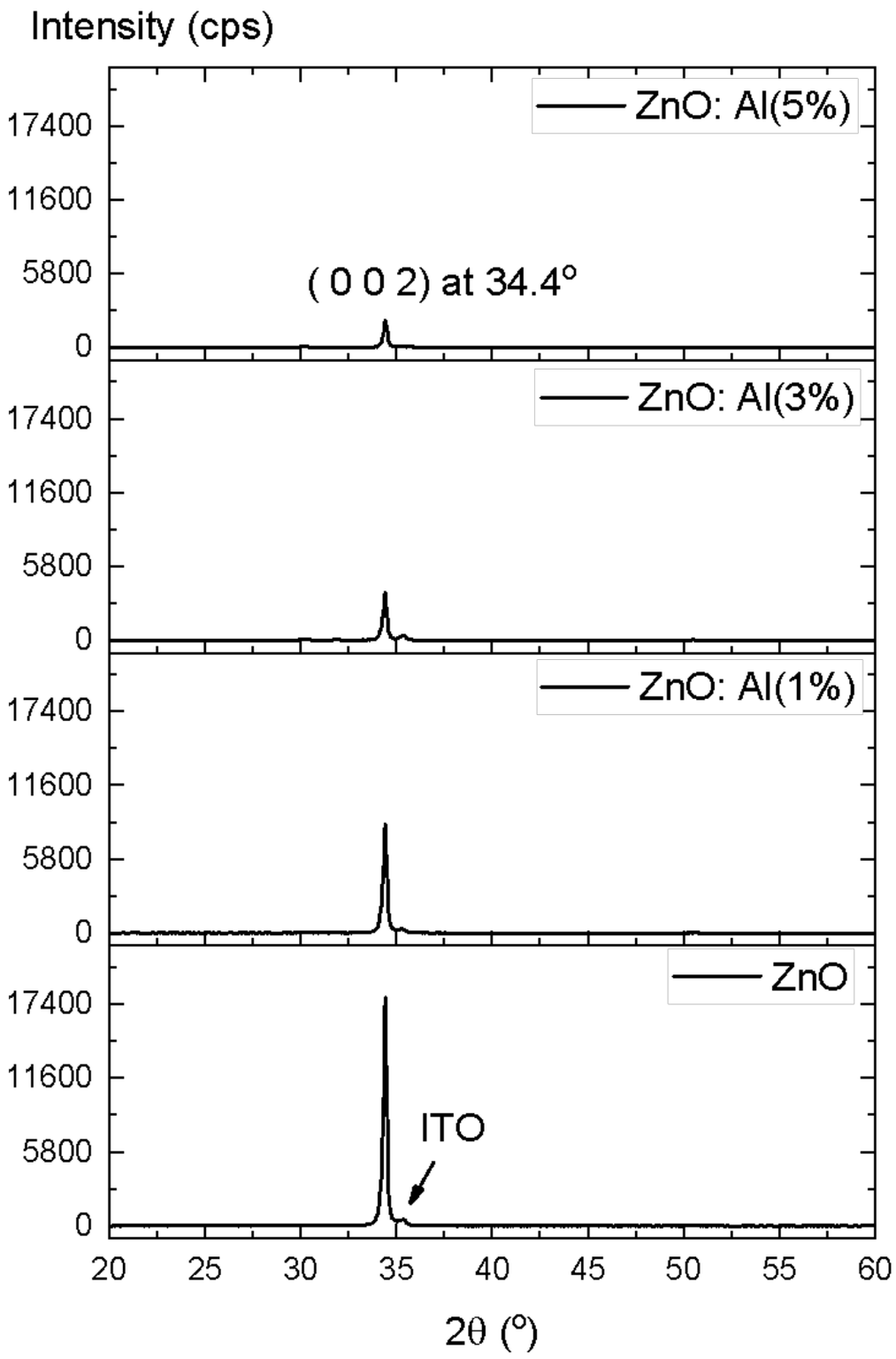

FIGURE 2. X-ray diffraction patterns of ZnO, ZnO:Al (1%), (3%) and (5%) of Al doped ZnO

result of the electrical double-layer capacitance produced by the hydration layer (Hsu & Chen 2010). Figure 5 shows the difference drift effect experiment result for the pH sensor. The drift rates of the pH sensor based on the ZnO were 7.97 mV/h. Notably, for ZnO:Al (1%), (3%), and (5%) were 3.43 mV/h, 2.82 mV/h, and 16.21 mV/h, respectively. Comparing the drift voltage among all the samples shows that ZnO:Al (3%) exhibited the highest stability, whereas ZnO:Al (5%) had the lowest stability. The binding strength was strengthened, and oxygen vacancies were compensated for by producing Al_2O_3 between the Al and oxygen atoms, reducing lattice defects, and resulting in a lower drift rate (Lee et al. 2013). Consequently, extrinsic ions could remove dangling bonds and modify for defects beneath the insulator membrane, resulting in improved performance. A large number of crystal defects might correlate with the higher drift rate (Al-Khalqi et al. 2021a; Kao et al. 2022; Tsai et al. 2019).

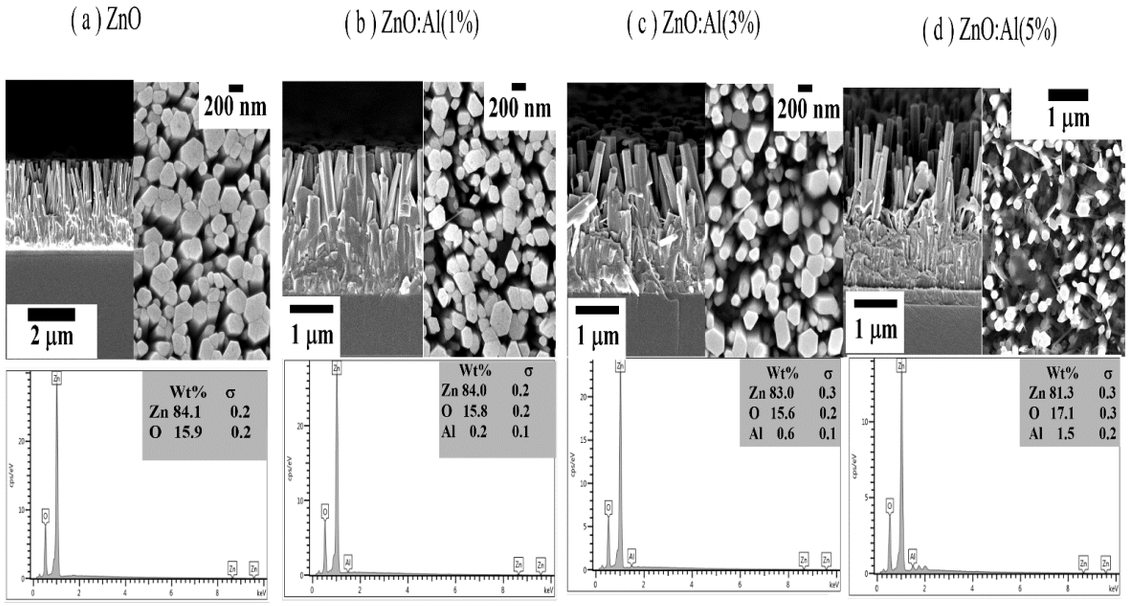

FIGURE 3. The FESEM hexagonal nanorods, cross section image and EDX spectrum of (a) ZnO, (b) ZnO:Al (1%), (c) ZnO:Al (3%) and (d) ZnO:Al (5%)

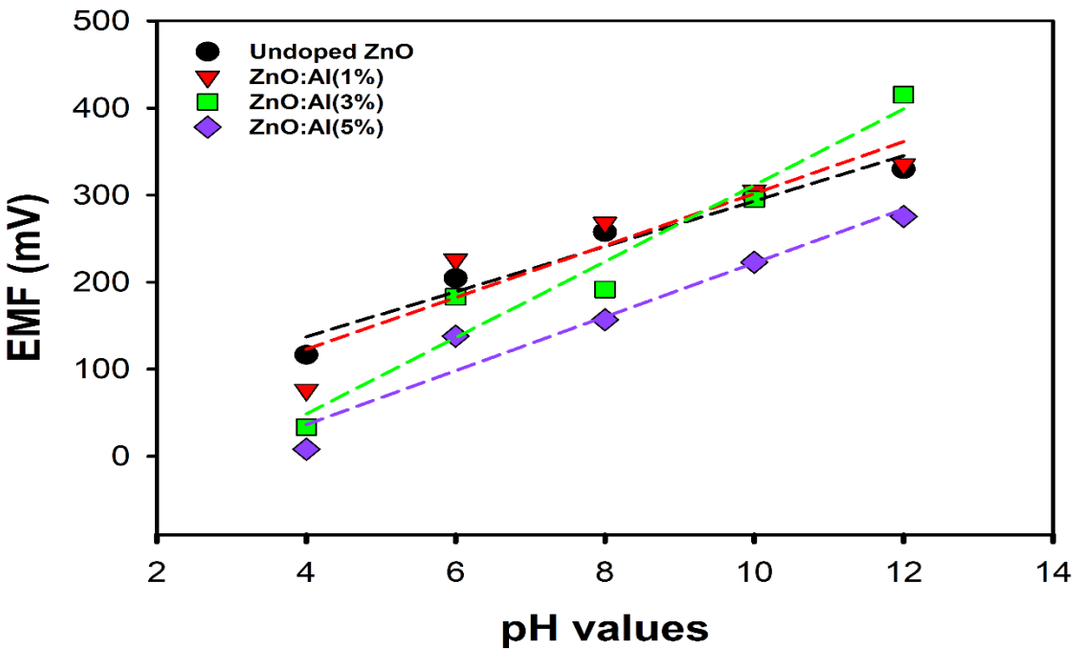

FIGURE 4. The response voltage with pH value in the range pH 4 to pH 12 of ZnO, ZnO:Al (1%), (3%) and (5%)

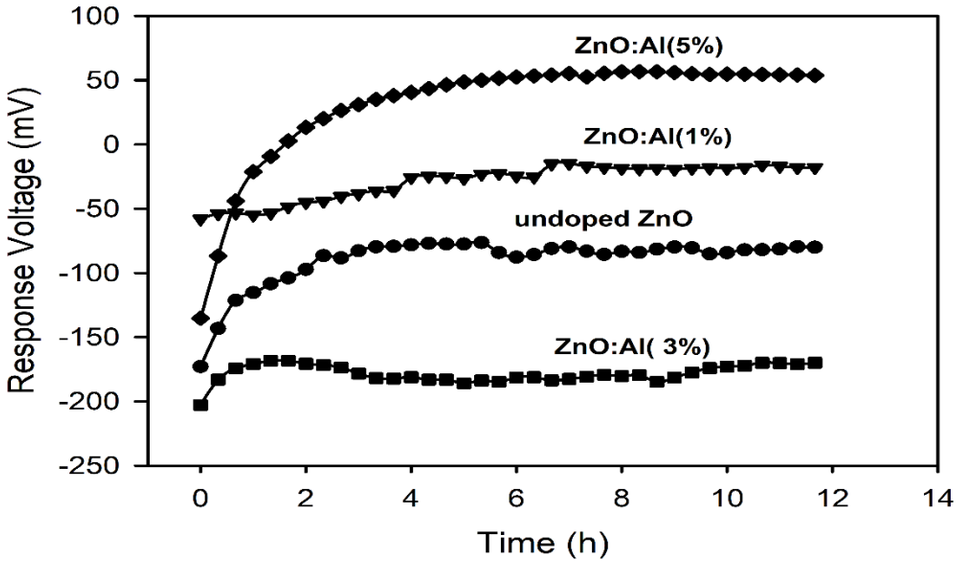

FIGURE 5. The drift rate of ZnO and ZnO:Al nanorods at 1%, 3% and 5%

CONCLUSION

In this study, we developed a pH sensor based on membranes made of ZnO and Al-doped ZnO nanorods for pH sensing characterization and Nerstian response voltage. The ZnO and ZnO:Al doping concentrations 1%, 3%, and 5% were controlled to provide the structure, morphology, and pH sensing properties. The pH sensor 3% ZnO:Al has been proven to have extraordinary sensing abilities, producing the highest sensitivity 43.80 mV/pH, with a linearity of 0.95, and exhibiting a lower drift rate behavior. By way of conclusion, with this technology, high-quality and Al-doped ZnO nanorods may be produced affordably for a range of cutting-edge applications.

ACKNOWLEDGEMENTS

This work was supported by Universiti Kebangsaan Malaysia (UKM) through short-term grant number GGPM-2020-039. The authors are also thankful to the Centre for Research and Instrumentation Management (CRIM) at UKM for providing the XRD, FESEM, and EDX measurements.

REFERENCES

Agarwal, M.B., Malaidurai, M., Sharma, A. & Thangavel, R. 2020. Effect of Al doping on hydrothermal growth and physical properties of doped ZnO nanoarrays for optoelectronic applications. *Materials Today: Proceedings* 21: 1781-1786.

Ahmed, S.M. 2018. Characterization of Al-doped ZnO nanorods grown by chemical bath deposition method. *Innovaciencia Facultad de Ciencias Exactas Físicas y Naturales* 6(1): 1-9.

Al Farsi, B., Al Marzouqi, F., Al-Maashani, M., Souier, M.T., Tay Zar Myint, M. & Al-Abri, M.Z. 2021. Rapid microwave-assisted fabrication of Al-doped zinc oxide nanorods on a glass substrate for photocatalytic degradation of phenol under visible light irradiation. *Materials Science and Engineering B: Solid-State Materials for Advanced Technology* 264: 114977.

Al-Hardan, N.H., Azmi Abdul Hamid, M., Firdaus-Raih, M. & Kar Keng, L. 2021. Aluminium - Modified Zno nanoparticles synthesized through Co-precipitation. *Jurnal Teknologi* 2: 1-6.

Al-Hardan, N.H., Hamid, M.A.A., Jalar, A., Shamsudin, R. & Othman, N.K. 2017. Synthesis of magnesium-doped ZnO rods via hydrothermal method: A study of the structural and optical properties. *ECS Journal of Solid State Science and Technology* 6(9): P571-P577.

Al-Khalqi, E.M., Hamid, M.A.A., Al-Hardan, N.H., Keng, L.K. & Jalar, A. 2022. Magnesium-doped ZnO nanorod Electrolyte–Insulator–Semiconductor (EIS) sensor for detecting organic solvents. *IEEE Sensors Journal* 22(12): 11783-11790.

Al-Khalqi, E.M., Hamid, M.A.A., Al-Hardan, N.H. & Keng, L.K. 2021a. Highly sensitive magnesium-doped zno nanorod ph sensors based on electrolyte–insulator–semiconductor (Eis) sensors. *Sensors* 21(6): 1-16.

Al-Khalqi, E.M., Hamid, M.A.A., Shamsudin, R., Al-Hardan, N.H., Jalar, A. & Keng, L.K. 2021b. Zinc oxide nanorod Electrolyte-Insulator- Semiconductor sensor for enhanced 2-methoxyethanol selectivity. *IEEE Sensors Journal* 21(5): 6234-6240.

Alkahlout, A., Al Dahoudi, N., Grobelsek, I., Jilavi, M. & de Oliveira, P.W. 2014. Synthesis and characterization of aluminum doped zinc oxide nanostructures via hydrothermal route. *Journal of Materials* 2014: 235638.

Belkhaoui, C., Mzabi, N., Smaoui, H. & Daniel, P. 2019. Enhancing the structural, optical and electrical properties of ZnO nanopowders through (Al + Mn) doping. *Results in Physics* 12(January): 1686-1696.

Ghazai, A.J., Salman, E.A. & Jabbar, Z.A. 2016. Effect of aluminum doping on zinc oxide thin film properties synthesis by spin coating method. *American Scientific Research Journal for Engineering, Technology, and Sciences (ASRJETS)* 26(3): 202-211.

Hashim, U., Fathil, M.F.M., Arshad, M.K.M., Gopinath, S.C.B. & Uda, M.N.A. 2017. Characterization of zinc oxide thin film for pH detector. *AIP Conference Proceedings*. p. 1808.

Hsu, C.H. & Chen, D.H. 2010. Synthesis and conductivity enhancement of Al-doped ZnO nanorod array thin films. *Nanotechnology* 21: 285603.

Kao, C-H., Liu, Y-W., Kuo, C-C., Chan, S-M., Wang, D-Y., Lin, Y.H., Lee, M.L. & Chen, H. 2022. Comparison of ZnO, Al_2O_3, AlZnO, and Al_2O_3-Doped ZnO Sensing membrane applied in electrolyte-insulator-semiconductor structures. *Membranes* 12(2): 168.

Kim, H., Piqué, A., Horwitz, J.S., Murata, H., Kafafi, Z.H., Gilmore, C.M. & Chrisey, D.B. 2000. Effect of aluminum doping on zinc oxide thin films grown by pulsed laser deposition for organic light-emitting devices. *Thin Solid Films* 377-378: 798-802.

Kumar, A., Naveen Kumar S.K., Aniley, A.A., Fernandez, R.E. & Bhansali, S. 2019. Hydrothermal growth of zinc oxide (ZnO) nanorods (NRs) on screen printed IDEs for pH measurement application. *Journal of The Electrochemical Society* 166(9): B3264-B3270.

Lee, C.H., Chuang, W.Y., Lin, S.H., Wu, W.J. & Lin, C.T. 2013. A printable humidity sensing material based on conductive polymer and nanoparticles composites. *Japanese Journal of Applied Physics* 52: 05DA08.

Liu, H., Zhou, Q., Zhang, Q., Hong, C., Xu, L., Jin, L. & Chen, W. 2017. Synthesis, characterization and enhanced sensing properties of a NiO/ZnO p–n junctions sensor for the SF6 decomposition byproducts SO_2, $SO2F_2$, and SOF_2. *Sensors (Basel)* 17(4): 913.

Mishra, P.N., Mishra, P.K. & Pathak, D. 2022. The influence of Al doping on the optical characteristics of ZnO nanopowders obtained by the low-cost sol-gel method. *Chemistry* 4(4): 1136-1146.

Naik, G.V., Liu, J., Kildishev, A.V., Shalaev, V.M. & Boltasseva, A. 2012. Demonstration of Al:ZnO as a plasmonic component for near-infrared metamaterials. *Proceedings of the National Academy of Sciences of the United States of America* 109(23): 8834-8838.

Peng, H., Wang, J., Lv, S., Wen, J. & Chen, J.F. 2015. Synthesis and characterization of hydroxyapatite nanoparticles prepared by a high-gravity precipitation method. *Ceramics International* 41(10): 14340-14349.

Porwal, A., Shafi, N. & Sahu, C. 2022. Fabrication and pH sensing characteristics measurement of back gate ZnO thin film planar FET. *Silicon* 14(17): 11687-11698.

Rayathulhan, R., Sodipo, B.K. & Aziz, A.A. 2017. Nucleation and growth of zinc oxide nanorods directly on metal wire by sonochemical method. *Ultrasonics Sonochemistry* 35: 270-275.

Tsai, Y.T., Chang, S.J., Ji, L.W., Hsiao, Y.J. & Tang, I.T. 2019. Fast detection and flexible microfluidic pH sensors based on Al-Doped ZnO nanosheets with a novel morphology. *ACS Omega* 4(22): 19847-19855.

Vavale, S.D., Pawar, S.G., Deshmukh, D.H. & Deshmukh, H.P. 2018. Hydrothermal method for synthesis of different nanostructure metal oxide thin film. *International Journal of Innovative Knowledge Concepts* 6(11): 126-129.

Wang, J.L., Yang, P.Y., Hsieh, T.Y., Hwang, C.C. & Juang, M.H. 2013. pH-sensing characteristics of hydrothermal Al-doped ZnO nanostructures. *Journal of Nanomaterials* 2013: 152079.

Yang, P-H., Chang, Y-S. & Chan, C-T. 2022. ZnO and AZO film potentiometric pH sensors based on flexible printed circuit board. *Chemosensors* 10(8): 293.

Yang, P.-Y., Wang, J.-L., Chiu, P.-C., Chou, J.-C., Chen, C.-W., Li, H.-H. & Cheng, H.-C. 2011. pH Sensing Characteristics of Extended-Gate Field-Effect Transistor Based on Al-Doped ZnO Nanostructures Hydrothermally Synthesized at Low Temperatures. *IEEE Electron Device Letters* 32(11): 1603-1605.

Young, S.J., Lai, L.T. & Tang, W.L. 2019. Improving the performance of pH sensors with one-dimensional ZnO nanostructures. *IEEE Sensors Journal* 19(23): 10972-10976.

Yue, J., Li, L., Cao, L., Zan, M., Yang, D., Wang, Z., Chang, Z., Mei, Q., Miao, P. & Dong, W.F. 2019. Two-step hydrothermal preparation of carbon dots for calcium ion detection. *ACS Applied Materials and Interfaces* 11(47): 44566-44572.

Zhang, Y., Wei, T., Dong, W., Huang, C., Zhang, K., Sun, Y., Chen, X. & Dai, N. 2013. Near-perfect infrared absorption from dielectric multilayer of plasmonic aluminum-doped zinc oxide. *Applied Physics Letters* 102: 213177.

Zheng, H., Zhang, R.J., Li, D.H., Chen, X., Wang, S.Y., Zheng, Y.X., Li, M.J., Hu, Z.G., Dai, N. & Chen, L.Y. 2018. Optical properties of Al-doped ZnO films in the infrared region and their absorption applications. *Nanoscale Research Letters* 13: 149.

*Corresponding author; email: kk@ukm.edu.my